

Northumbria Research Link

Citation: Li, Hou-Chang, Wang, Meng-Yu, Liu, Bin, Liu, Juan, Wang, Qi, He, Xing-Dao, Ping Chan, Hau, Wang, Danling, Yuan, Jinhui and Wu, Qiang (2022) Temperature-independent relative humidity sensing properties of polymer micro-bottle resonators coated with graphene oxide. *Measurement*, 196. p. 111199. ISSN 0263-2241

Published by: Elsevier

URL: <https://doi.org/10.1016/j.measurement.2022.111199>
<<https://doi.org/10.1016/j.measurement.2022.111199>>

This version was downloaded from Northumbria Research Link:
<https://nrl.northumbria.ac.uk/id/eprint/49022/>

Northumbria University has developed Northumbria Research Link (NRL) to enable users to access the University's research output. Copyright © and moral rights for items on NRL are retained by the individual author(s) and/or other copyright owners. Single copies of full items can be reproduced, displayed or performed, and given to third parties in any format or medium for personal research or study, educational, or not-for-profit purposes without prior permission or charge, provided the authors, title and full bibliographic details are given, as well as a hyperlink and/or URL to the original metadata page. The content must not be changed in any way. Full items must not be sold commercially in any format or medium without formal permission of the copyright holder. The full policy is available online: <http://nrl.northumbria.ac.uk/policies.html>

This document may differ from the final, published version of the research and has been made available online in accordance with publisher policies. To read and/or cite from the published version of the research, please visit the publisher's website (a subscription may be required.)

Measurement

Temperature-Independent Relative Humidity Sensing Properties of polymer Micro-bottle Resonators Coated with Graphene Oxide --Manuscript Draft--

Manuscript Number:	MEAS-D-22-00312R1
Article Type:	Research Paper
Keywords:	Keywords: relative humidity; micro-bottle resonator; polymer material; whispering-gallery Mode (WGM); Graphene oxide
Corresponding Author:	Bin Liu, Ph.D. Nanchang Hangkong University Nanchang, China CHINA
First Author:	Hou-Chang Li
Order of Authors:	Hou-Chang Li Meng-Yu Wang Bin Liu, Ph.D. Juan Liu Qi Wang Xind-Dao He Hau Ping Chan Danling Wang Jinhui Yuan Qiang Wu
Abstract:	<p>A polymer-based micro-bottle resonator coated with graphene oxide (GO) film is presented to improve the relative humidity (RH) sensing performance. Polymeric material Loctite 3525 was coated onto a quartz fiber and cured by using UV light irradiation and thermal reflow technology. A layer of GO film was prepared on the resonator by the dip impregnation method, which realized a high Q-factor ($>10^4$) transmission of energy by appropriately designing a wave-guide resonator coupling. By optimizing the concentration of GO, high sensitivity and figure of merit (FoM) of 0.161 and 2.01/%RH were achieved in the RH range of 22~81%. After high-temperature annealing at 300 °C, the temperature sensitivity decreased by an order of magnitude from 0.793 to 0.068 nm /°C, which significantly reduces the cross-sensitivity between humidity and temperature. The proposed resonator has the advantages of being compact in size, low in cost, high sensitivity, and low in temperature crosstalk.</p>

Temperature-Independent Relative Humidity Sensing Properties of polymer Micro-bottle Resonators Coated with Graphene Oxide

Abstract

A polymer-based micro-bottle resonator coated with graphene oxide (GO) film is presented to improve the relative humidity (RH) sensing performance. Polymeric material Loctite 3525 was coated onto a quartz fiber and cured by using UV light irradiation and thermal reflow technology. A layer of GO film was prepared on the micro-bottle resonator by the dip impregnation method, which realized a high Q-factor ($>10^4$) transmission of energy by appropriately designing a wave-guide resonator coupling. By optimizing the concentration of GO dip impregnation solution, high sensitivity and figure of merit (FoM) of $0.161 \text{ nm}/\% \text{RH}$ and $2.01/\% \text{RH}$ were achieved in the RH range of 22~81%. In addition, after high-temperature annealing at $300 \text{ }^\circ\text{C}$, the temperature sensitivity decreased by an order of magnitude from $0.793 \text{ nm}/^\circ\text{C}$ to $0.068 \text{ nm}/^\circ\text{C}$, which significantly reduces the cross-sensitivity between humidity and temperature. The proposed resonator has the advantages of being compact in size, low in cost, high sensitivity, and low in temperature crosstalk.

Keywords: relative humidity; micro-bottle resonator; polymer material; whispering-gallery mode (WGM); graphene oxide

1. Introduction

Humidity is one of the most accessible physical forces in daily life. People's dietary activities and the survival and reproduction of animals and plants are closely related to the humidity of the environment. With the development of the social economy, all walks of life have more and more strict requirements on humidity indicators, and the requirements on all aspects of humidity sensors are getting higher and higher. The use of traditional humidity sensors in some extreme environments will be restricted, but fiber optic sensors have the advantages of anti-electromagnetic interference, high sensitivity, lightweight, small size, corrosion resistance, and electrical insulation [1], [2]. Therefore, the optical fiber humidity sensor has attracted more and more researchers' attention.

Since the material of the optical fiber itself is not sensitive to humidity, most optical fiber humidity sensors need to be coated with a moisture-sensitive coating on the surface of the optical fiber to enhance the humidity-sensitive characteristics of the optical fiber sensor. Common humidity-sensitive materials mainly include gelatin (Gelatin) [3], polyvinyl alcohol (PVA) [4], tungsten disulfide (WS_2) [5], zinc oxide (ZnO) [6], titanium dioxide (TiO_2) [7], carbon nanotubes (Carbon nanotubes) [8], etc. Among them, GO [9-11] is considered to be an excellent humidity sensitizing material because of its unique photoelectric properties, high sensitivity to external environmental changes, and strong adsorption capacity for water molecules. Based on this, people have designed a variety of fiber optic humidity sensors with different structures, such as fiber grating humidity sensors [12], resonant cavity humidity sensors [13], interferometric humidity sensors [14], and so on. Among them: the grating-type humidity sensor has a stable structure, but its sensitivity is generally low due to objective factors of its sensing principle; the humidity sensor has the advantage of high sensitivity, but the disadvantage is that some have complex structures, difficult production, and some are expensive. In recent years, with the improvement of the micro-machining level and the emergence of new processing techniques, WGM micro-cavities of various geometries have been fabricated and extensively studied. Sensors based on WGM can provide a very long photon lifetime and high Q-factor. This makes it an ideal humidity sensor for many applications. For example, in 2016, Ahmad [15] *et al.* pulled a common single-mode fiber (SMF-28) into a micro-nano fiber with a diameter of $4.04 \text{ } \mu\text{m}$. On this basis,

the micro-nano fiber was made into a micro-nano fiber ring resonator (MLR) and covered the surface of MLR with GO film. The sensitivity is $0.0537 \text{ nm}/\% \text{RH}$ in the range of 30 % to 50 % RH. However, the ring resonant cavity humidity sensor prepared based on micro-fibers has a complicated preparation process and is not conducive to the coating of humidity-sensitive materials, which limits the improvement of its sensitivity. In addition, the limitation of measurement types caused by cross-sensitivity has always been a problem that plagues the integration of optical fiber sensing systems. The multimodal method [16] is an effective method to solve the cross-sensitivity problem. However, the number of resonance peaks with different sensitivities is limited, and the merit value is low, resulting in low measurement types and resolution. Therefore, there is an urgent need for a humidity sensor with small effective sensing volume, low-temperature crosstalk, and high FoM.

Based on previous research, this paper designs and manufactures a micro-bottle resonator humidity sensor using polymer material (Loctite 3525) composite GO film. Loctite 3525 is a commercial UV-sensitive material that cures to a depth of 1 cm at low irradiance ($30\text{-}50 \text{ mW}/\text{cm}^2$) at 365 nm . The total light transmittance of the material after curing is greater than 99 %, and the transparency is close to that of optical glass, so it is very suitable for micro-resonators. By combining with GO, humidity sensing with a sensitivity of $0.161 \text{ nm}/\% \text{RH}$ is realized. In addition, the high-temperature annealing technology ($300 \text{ }^\circ\text{C}$) eliminates the influence of temperature on the RH sensor and achieves the purpose of temperature insensitivity, thereby improving the accuracy of humidity measurement. The designed humidity sensor has the advantages of high Q-factor, high-sensitivity, and low-temperature crosstalk. It has certain application prospects in analytical chemistry, environmental monitoring, and other fields.

2. Theoretical analysis

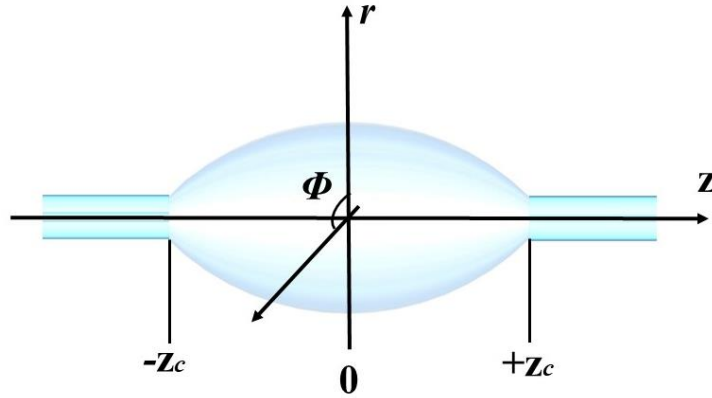


Fig. 1. Schematic diagram of the structure of the micro-bottle resonator

The micro-bottle resonator satisfies the cylindrical symmetry distribution (Fig. 1). Considering the mode distribution characteristics, the solution needs to be carried out in a cylindrical coordinate system. First, we perform numerical modeling on the micro-bottle cavity structure. Assuming that the cavity shell is parabolic:

$$R(z) \approx R_0 \left(1 - \frac{1}{2(\Delta K \cdot Z)^2} \right) \quad (1)$$

Where R_0 is the maximum radius of the cavity at $Z = 0$, which ΔK is the curvature of the cavity profile. The electric and magnetic fields follow the Helmholtz equation:

$$\begin{aligned} (\nabla^2 + k^2) \cdot \vec{E} &= 0 \\ (\nabla^2 + k^2) \cdot \vec{H} &= 0 \end{aligned} \quad (2)$$

In cylindrical coordinates, the Laplacian has the following form:

$$\nabla^2 = \frac{1}{r} \partial_r + \partial_r^2 + \frac{1}{r^2} \partial_\phi^2 + \partial_z^2 \quad (3)$$

Since the radius of the micro-bottle resonator in the axial z -direction is very small, it satisfies $dR/dz \ll 1$. The propagation wave vector kr in the radial component is negligible relative to the other two directions. The projection component in the z -direction is a constant value, there is $\partial_z k_\phi(z)R(z) = 0$. The propagation wave-vector will disappear at a special position in the axial component. This position is recorded as $\pm Z_c$, which is called the axial cutoff point $k_z(\pm Z_c) = 0$. The components of k in the other two directions are converted to:

$$k_\phi(z) = \frac{kR_c}{R(z)} \quad (4)$$

$$k_z(z) = \pm k \sqrt{1 - \left[\frac{R_c}{R(z)} \right]^2} \quad (5)$$

Approximately under adiabatic conditions, separating the variables of the wave equation, according to formula (2), the Helmholtz equation can be further rewritten as:

$$(\nabla^2 + k^2) \cdot \phi(r, R(z))Z(z)e^{im\phi} \quad (6)$$

Where $\phi(r, R(z))$ is the radial wave function, and $Z(z)$ is the Z -direction (axial) wave function. Separate the variables of the equations to obtain the radial wave equation and the axial wave equation respectively. When they are solved separately, we can get:

$$\Phi_m(r, z) = \begin{cases} A_m J_m(k_\phi r) & , r < R(z) \\ H_m^{(2)}\left(\frac{k_\phi r}{n}\right) + B_m H_m^{(1)}\left(\frac{k_\phi r}{n}\right) & , r > R(z) \end{cases} \quad (7)$$

In the formula, $\Delta E_m = 2m\Delta k/R_0$, where $H_m^{(1,2)}$ is the Hankel function, A_m, B_m is the coefficient determined by the boundary continuity condition. H_q is the Hermitian polynomial of order q , $C_{mq} = [\Delta E_m / (\pi 2^{2q+1} (q!)^2)]^{1/4}$. At this point, we have obtained the axial and radial field distribution of the micro vial cavity. If you need to further obtain the TE (TM) mode distribution, apply boundary continuity conditions ($H_z, E_\phi(H_\phi, E_z)$) and its derivatives to obtain their resonance conditions, and then bring them back to eqs. (1) and (2).

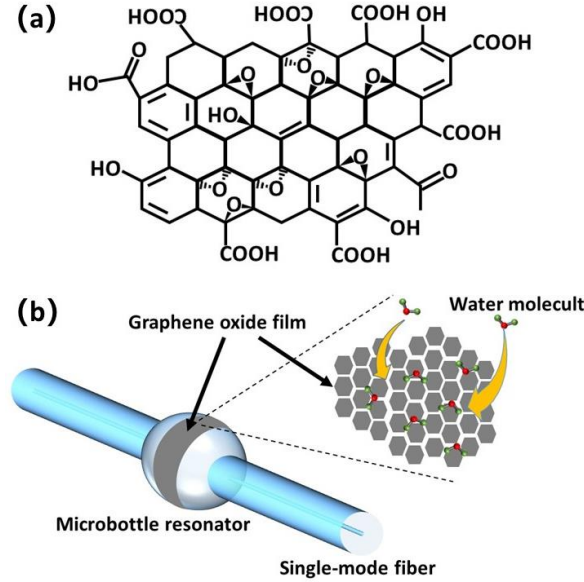


Fig. 2. (a) GO molecular structure (b) GO interacting with water molecules

GO is a two-dimensional material with a honeycomb structure (Fig. 2(a)), and the large oxygen-containing functional groups (such as -COOH and -OH) are covalently bonded between layers or on the boundary so that GO has good dispersibility and

hydrophilicity. Studies have shown that water molecules play a key role in maintaining the layered structure of GO. Through neutron scattering experiments, it is more certain than the water molecules are through the interaction between the oxygen in the epoxy groups on the surface of GO and the hydrogen bonds in the water molecules [17]. And the physical adsorption caused by van der Waals forces and hydrogen bonds ensures that water molecules are adsorbed and fixed on the surface of the GO film (Fig. 2(b)). In addition, there are more active carriers on the surface of the GO film, which can easily adsorb water molecules, and the adsorbed water molecules will become the carriers of the next layer [18]. As the ambient RH increases, the formants also change. This can be explained that when the surrounding RH increases, the GO coating absorbs more water from the environment, increasing the distance between the GO layers [19]. In addition, charge transfer occurs between the GO film and water molecules reducing the effective RI of the GO coating [20]. These two factors together lead to changes in light absorption, which in turn affect the intensity and wavelength shift of the light field.

3. Fabrication of the sensor

The method for manufacturing a bottle-shaped resonator is shown in Fig. 3. Firstly, prepare a piece of standard single-mode fiber (SMF-28e, Corning) as a bracket and place it on two three-axis translational stages. Then, a polymer solution was coated onto the optical fiber, and the polymer will reflow into the shape of a micro bottle. This behavior depends on the performance parameters of Loctite 3525 itself (Table 1). Finally, it was cured with Ultraviolet light (SPCM-0800, China), and the temperature control box was heated (about 300 °C and 10 seconds). After the stable micro-bottle cavity structure is formed, its surface morphology needs to be further processed by thermal reflow technology. By reheating the polymer to a micro-melt state, the processing defects on the surface are repaired, and the surface form GO nano-film on the surface of the micro-cavity and dry (30°C) for about 4 hours finish is improved, to achieve the purpose of reducing the transmission loss of the polymer and improving the performance of the resonant cavity [21].

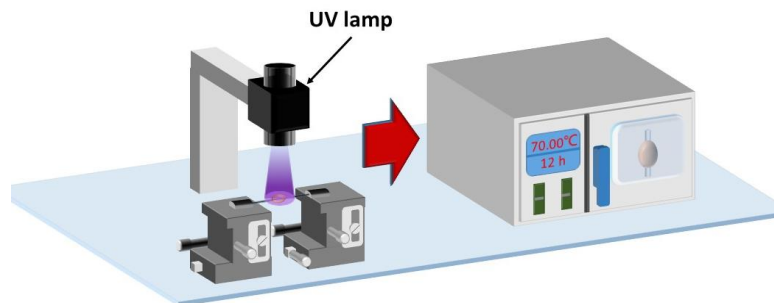


Fig. 3. UV curing and high-temperature thermal reflow device

TABLE 1
PROPERTIES VALUES OF POLYMER MATERIALS

Polymer material	Sensitivity					
	RI	Viscosity (cps)	Hardness (Shore)	Young's modulus [mpa]	Elongation (%)	Thermal expansion coefficient (ppm/□)
Loctite3525	1.51	15000	DA68	25	160	120

To further realize humidity sensing, a GO film was fabricated on the surface of the micro-bottle resonator using the modified Hummer method [22]. The process is shown in Fig. 4:

- I. Micro-bottle resonator was cleaned with alcohol before coating;
- II. GO is dispersed in the solvent of deionized water by ultrasound, the GO solution with a concentration of about 0.001, 0.01 and 0.1 mg/ml are centrifuged in ultrasound for 30 min (70 °C) and obtain uniform GO crystal suspension;

III. Then the micro-bottle resonator was impregnated with GO solution for 0.5 h;

IV. To obtain a uniform solid GO nano-film, a micro-bottle resonator was dried in a drying oven at 30 °C for 4 h.

Different from the quartz crystal microbalance sensor based on GO film [23], the thickness of GO nano film coated by the evanescent wave optical sensor is relatively thin. Stirring or sonication can get a uniform and stable GO dispersion liquid for the good dispersibility of GO in water. Three different low concentrations GO dispersion liquid (0.001, 0.01 and 0.1 mg/ml) were prepared by stirring or sonication, which were drop coated on the surface of micro-bottle cavity to form GO nano-film. Field emission scanning electron microscopy (FESEM, FEI Nanosem 450*) images of micro-bottle cavity coated with 0.001, 0.01 and 0.1 mg/ml GO are shown in Fig. 5.

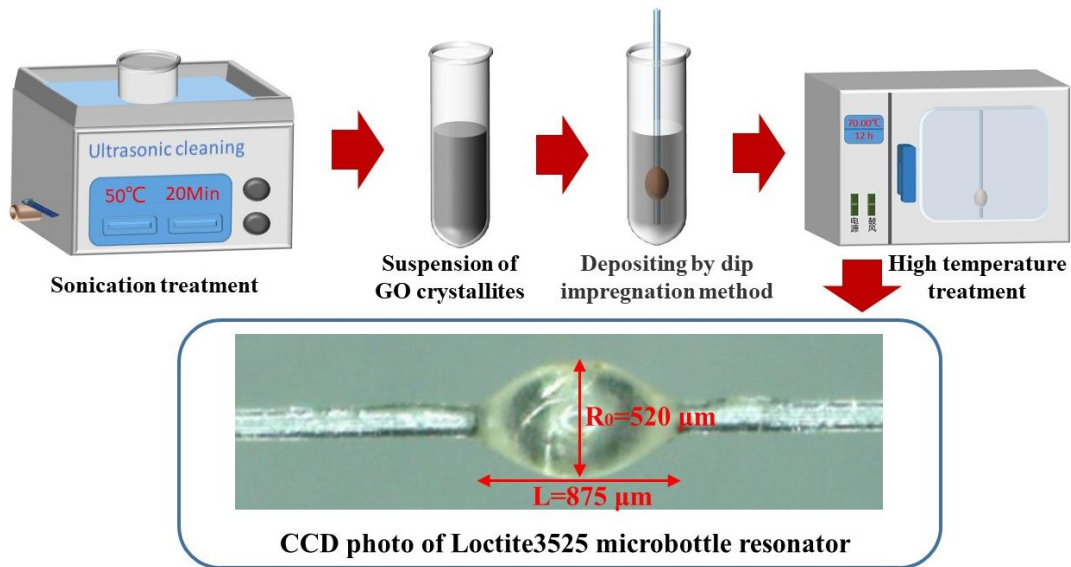


Fig.4. The manufacturing process of GO film

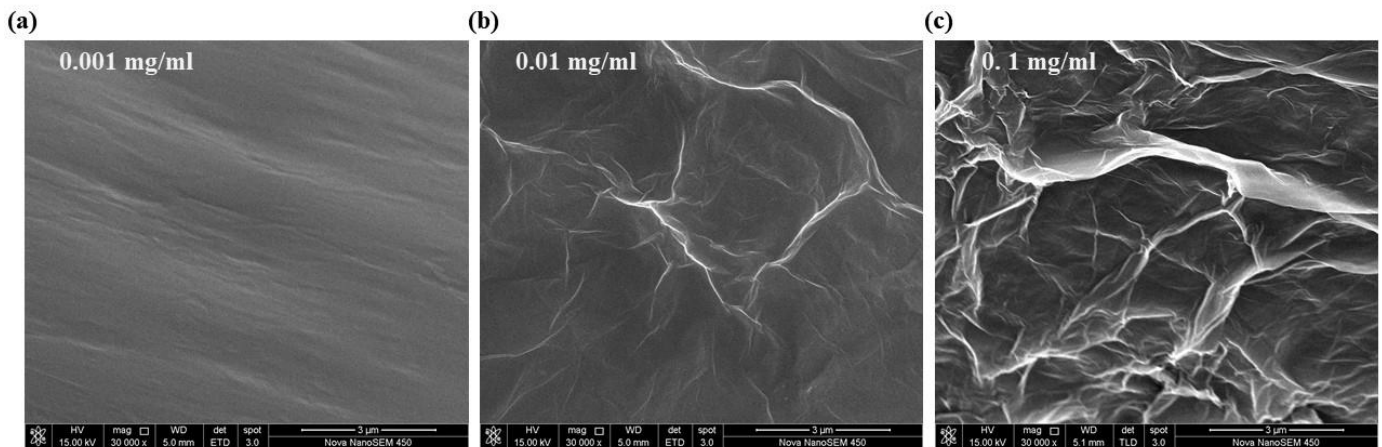


Fig. 5. SEM images of the micro-bottle cavity coated with GO (a) 0.001 mg/ml (b) 0.01 mg/ml (c) 0.1 mg/ml.

4. Experimental results and analysis

A fiber-optic tapered wave-guide coupling system was built to test the resonant spectral characteristics of the micro-bottle resonator, as shown in Fig. 6. The coupling between the micro-cavity and wave-guide fiber is precisely controlled by two three-dimensional adjustment frames (MBT610D) with a resolution of 50 $\mu\text{m}/\text{rev}$ (300 μm Range). Use a CCD (AO-UV200) to observe the position between the tapered fiber and micro-bottle resonator. Then, the light emitted by the light source (BBS, ASE-C-30-B, Hefei Max-ray Photonics) is coupled into the micro-cavity by wave-guide fiber. The output optical signal was recorded by a

spectrometer (OSA, Yokogawa AQ6370D). Fine-tune the position between the micro-cavity and wave-guide fiber, and encapsulate it when an ideal and stable transmission spectrum is obtained.

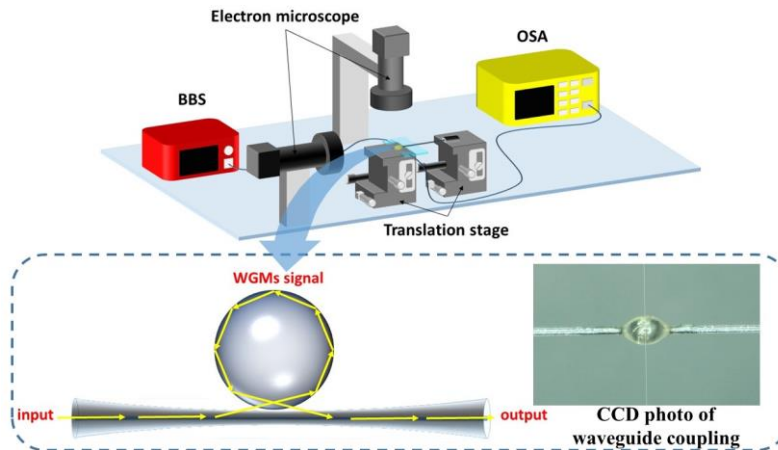


Fig. 6. Wave-guide coupling and encapsulation.

Using the tapered fiber wave-guide coupling with a taper waist diameter of $2.4 \mu\text{m}$, the micro-bottle resonator with dimensions $R_0 = 520 \mu\text{m}$, $L = 875 \mu\text{m}$ was tested. When the coupling point of the fiber tapered waveguide is located in the center of the micro-bottle resonator, the excited resonance spectrum is shown in Fig. 7(a). It can be seen that due to the existence of radial mode and axial mode in the micro-bottle resonator, the light takes a spiral route in the micro-bottle resonator, and the azimuthal mode will appear degenerate, so the resonance spectrum of the micro-bottle resonator is extremely dense. The free spectral range (FSR) between two adjacent mode numbers is marked in the figure, which is about 1.33 nm . The FSR is inversely proportional to the radius of the micro-cavity, and the larger the size, the smaller the FSR. When the micro-cavity is used for sensing applications, it is usually desirable to obtain a large FSR to increase the detection range in sensing applications. In addition, the Q-factor is a key parameter to measure the resonant performance of a resonator, and it is also a manifestation of the energy storage capacity of the resonator. This value is related to the optical energy stored in the resonator and the optical power loss when the light rotates a circle inside the resonator. Generally, the Q-factor can be obtained by calculating the half-maximum value (FWHM) in a specific experimental measurement [24], and the calculation formula is as follows:

$$Q = \frac{\lambda}{FWHM} \quad (9)$$

The experimentally measured transmission spectra of the micro-bottle resonator at different concentrations (0.001 mg/ml and 0.5 mg/ml) are shown in Fig. 7(c) and (d), and the peak fitting was performed with Lorentzian profiles. Its optical mode FWHM From 0.03 nm to 0.27 nm , the corresponding optical quality factor decreases from 5.326×10^4 to 5.9×10^3 , that is, the Q-factor decreases with the increase of graphene concentration, and its downward trend is shown in Fig. 7(b). The results showed that even at a very high concentration ($>0.5 \text{ mg/ml}$), the Q-factor was reduced by only one order of magnitude. This makes GO a very suitable moisture-sensitive material for this micro-bottle resonator.

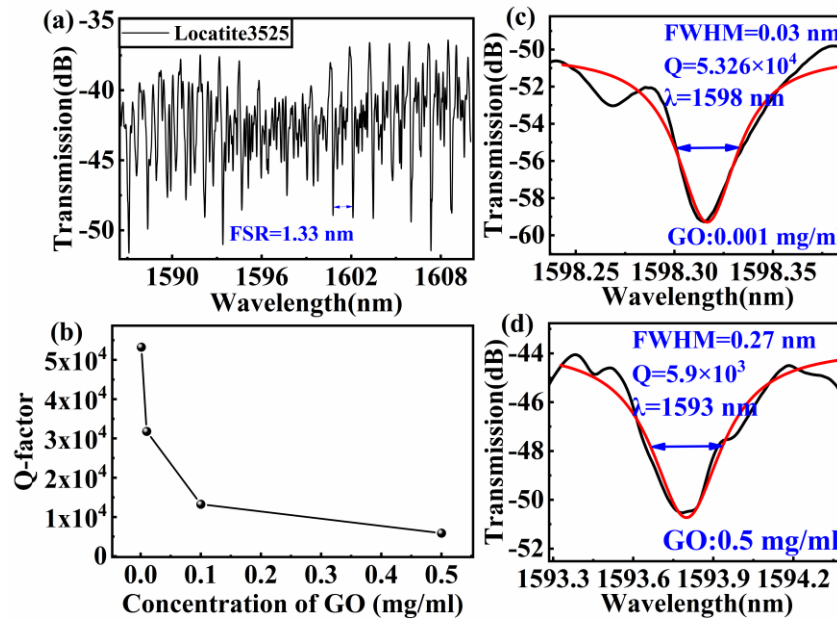


Fig. 7. (a) Transmission spectrum of Locatite 3525. (b)-(d) Q-factor corresponding to different GO concentrations.

Three different concentrations of GO (0.001, 0.01, and 0.1 mg/ml) solutions were prepared using the same micro-bottle chamber samples for humidity measurement. The experimental setup of the humidity test system is shown in Fig. 8. The sensor was fixed on the shelf of a programmable humidity test box (ST-80L, Xiamen Yishh Instrument Co. Ltd.) to ensure the stability and mechanical properties of the fiber structure. The chamber is thermoelectrically controlled to ensure measurement at a constant temperature. Both ends of the sensor go out of the chamber via optical fibers and connect to the BBS and OSA connections. Data were recorded for each humidity gradient spectrometer to study the relationship between center wavelength and humidity.

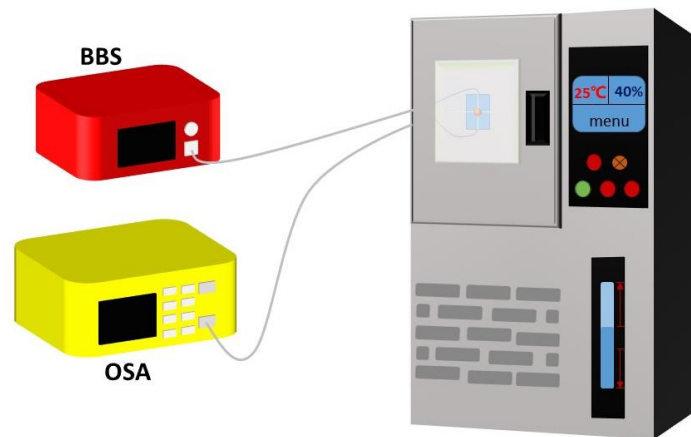


Fig. 8. Schematic diagram of the RH experimental setup.

Figures 9(a)-(c) show the transmission spectra of the three samples with the change of the RH of the external environment. It can be seen from the figure that when the RH of the external environment increases, the resonance wavelengths of all three samples were red-shifted. This is due to the increase in the RH, the water molecules occupy the effective active sites of the GO films. The layer of water molecules adsorbed on the surface of the GO film gradually exhibits the properties of liquid water. Water molecules penetrate the middle layer of the GO film, increasing the distance between the GO layers. In addition, the absorption of water

molecules leads to charge transfer between the GO film and the water molecules. When the water molecules are adsorbed to the epoxy groups, the charge density between the hydrogen atoms in the water molecules and the oxygen atoms of the epoxy groups increases. Meanwhile, the carbocyclic ring connected to the hydroxyl group also has a small amount of charge transfer, and there is also a charge increase in the benzene ring below the OH bond of the water molecule. The interlayer distance and dielectric constant variation of GO films can affect the effective RI through evanescent waves propagating in the micro-bottle cavity, resulting in a wavelength shift of the interference fringes during transmission. During the process of increasing the humidity from 20% RH to 80% RH [Fig. 9(d)], the corresponding microcavities with three different concentrations of 0.001, 0.01 and 0.1 mg/ml, the sensitivities were 0.04, 0.161 and 0.068 nm/%RH, respectively. The experimental results show that the humidity sensitivity brought by different concentrations of GO is slightly different. In the same conditions, the sensitivity of the sensor first increases and then decreases with the increase of the thickness of the humidity-sensitive film. The greater the wavelength change, the higher the sensitivity. However, when the thickness of the humidity-sensitive film exceeds a certain thickness, although the thicker the humidity-sensitive film can absorb more water molecules, the transmission of external water molecules to the interior of the humidity-sensitive film is affected by the thickness [25], which makes it difficult for the light beam transmitted inside the humidity-sensitive film to respond to the external humidity change information, and the sensitivity of the sensor decreases. It can be seen that when the GO concentration is about 0.01 mg/ml, the RH sensitivity in the range of 20% RH to 80% RH is the largest, and the maximum sensitivity is -0.161 nm/% RH. In addition, the sensor before coating GO was measured, and the interference peak hardly moved with the increase of humidity. This is due to the weak influence of the change of RI around the sensor area on the evanescent field.

In most sensors, sensitivity (S) and FoM are important parameters to evaluate their sensing performance. In actual sensing applications, the narrow line-width resonance dip is conducive to accurate detection. Therefore, the FoM coefficient is more meaningful than the S coefficient. Can be expressed as:

$$FOM = \frac{S}{FWHM} \quad (10)$$

Compared with the traditional optical fiber sensor structure, the WGM has a good Q-factor and can achieve a relatively high FoM (2.01/%RH). Such as, in 2020, Petra Urbancova *et al.* [26] proposed a new guided-mode resonance (GMR) humidity sensor based on the use of a planar waveguide structure (PWS), with an FoM of 3.7×10^{-3} /%RH. In 2021, Zixian Hu *et al.* [27] an ultra-small fiber-optic microprobe Fabry-Perot interferometer (FPI) RH sensor is proposed, with FoM~0.95/%RH.

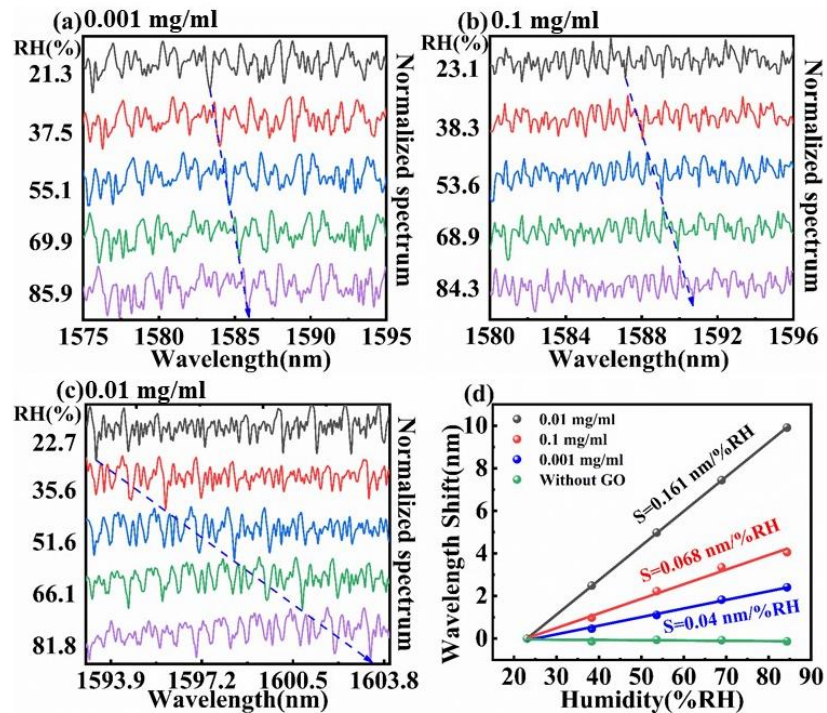


Fig. 9. (a)-(c) The changing trend of the transmission spectrum with humidity (0.001, 0.1, and 0.01 mg/ml (GO)) (d) The linear fitting results of different concentrations of GO.

Temperature crosstalk is generally associated with humidity measurements, so the structure was temperature tested. The experiment compared the spectra of the sensor before and after annealing at 25-29 °C [Fig. 10(a) and (b)]. The temperature response sensitivity before and after annealing is $0.793 \text{ nm}/\square$ and $0.068 \text{ nm}/\square$, respectively, significantly reducing the temperature sensitivity of the sensor. This property may be related to the structure of the material itself, according to the Material Safety Data Sheet (MSDS), Loctite 3525 is an acrylic resin [28]: including polyurethane methacrylate resin, hydroxyethyl methacrylate, methacrylate, and diphenyl-2, 4, 6-trimethyl benzyl. These substances are divided into two free radicals during the polymerization process and then incorporated into the polymer as chain ends. High-temperature annealing eliminates the unsaturated double bonds at the head and end of the unstable structure of acrylic resin polymer, thereby improving the thermal stability of the sensor [29]. Moreover, the humidity response characteristics of the sensor at different temperatures (25 °C and 35 °C) were investigated experimentally. When the GO concentration was 0.01 mg/ml, the sensitivity was $0.161 \text{ nm}/\%RH$ and $0.167 \text{ nm}/\%RH$, respectively [Fig. 10(c)]. The increased sensitivity of the GO sensor is possibly due to the increase in absolute vapor pressure with increasing temperature, thus adsorbing more water molecules [30]. Since the thin films we form using low concentrations of GO are relatively thin, temperature changes have less effect on humidity sensing.

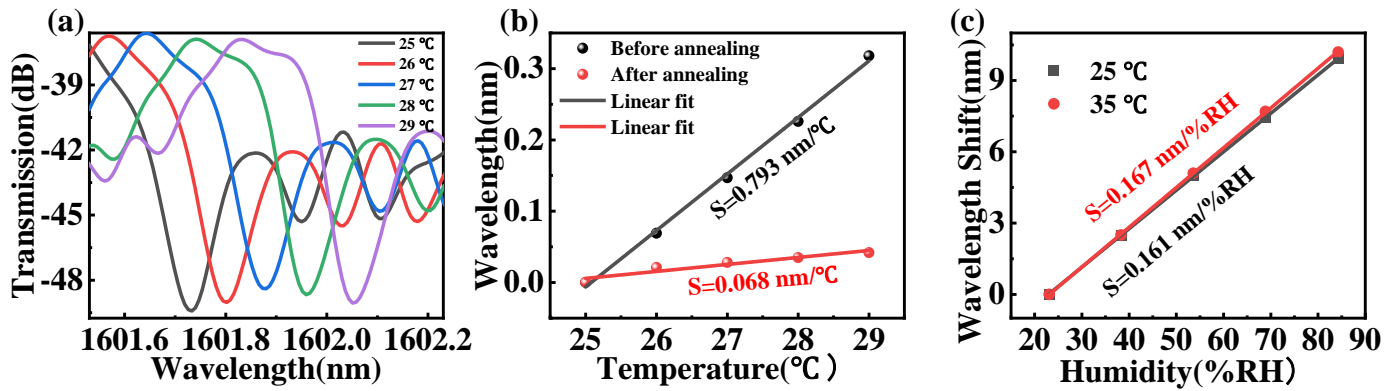


Fig. 10 (a) The spectral response of the resonator in the temperature range of 25-29 °C was measured; (b) The temperature sensitivity of the sensor before/after annealing; (c) The humidity response at different temper.

For Loctite 3525, compared with other humidity sensors based on WGM reported in the literature. In a larger humidity measurement range, it shows excellent performance, as shown in table 2.

TABLE 2
PERFORMANCE OF OTHER RH SENSORS REPORTED.

Structure	Material	Measurement range(%RH)	Sensitivity (nm/%RH)	Ref.
Micro-toroid (WGM)	Silica and pNIPAAm	-	0.012	[31] (2013)
Micro-cavity (WGM)	Roll up Polymer/oxide/polymer nanomembranes	5-97	0.13	[32] (2014)
An embedded silica optical microfiber knot resonator	Nafion	30-45	0.11 ± 0.02	[33] (2014)
		45-75	0.29 ± 0.01	
Micro-disk (WGM)	SU-8 polymer	0-5	0.078	[34] (2017)
		45-50	0.023	
Micro-sphere (WGM)	Silica and Agarose hydrogel	1-25	0.0007	[35] (2018)
Fabry-Perot interferometer and Bragg grating (FBG)	polyimide (PI)	35-65	0.986	[36] (2018)
Micro-spheres (WGM)	PMMA	-	0.047	[37] (2018)
Microfiber knot resonators (MKRs)	GO	0-80	0.0104	[38] (2018)
Microfiber knot resonators (MKRs)	Not Available	28.6-53.4	0.01	[39] (2019)
Micro-sphere (WGM)	ZnO	35-85	0.014	[40] (2021)
Micro-bottle (WGM)	Loctite3525 and GO	22-81	0.16	This paper

5. Conclusion

This paper proposed a micro-bottle resonator made of polymer (Loctite 3525) by UV curing and high-temperature treatment. The surface of the micro-bottle resonator is coated with a layer of GO film and realizes high sensitivity humidity sensing. High Q-factor (10^4) transmission spectrum obtained through the straight wave-guide coupling of micro-fiber. The micro-bottle resonator exhibits a high RH sensitivity of $0.161 \text{ nm}/\%RH$ and good stability in RH sensing with optimizing the concentration of the dip impregnation GO solution. The extremely narrow line-width of WGM improves the FoM of the sensor, which reached $2.01/\%RH$.

The thermal stability of polymer materials is improved by high-temperature treatment, the temperature sensitivity of the micro-bottle resonator is reduced by an order of magnitude which humidity sensing with low-temperature crosstalk is realized. The proposed sensor design has the advantages of higher sensitivity, better stability, simpler structure, and low-temperature crosstalk, and has certain practical application prospects.

Acknowledgements

This work was jointly supported by National Natural Science Foundation of China (NSFC) (11864025, 62065013, 61865013, 62175097); Natural Science Foundation of Jiangxi Province (Grant No. 20212BAB202024 and 20192ACB20031), Key R&D Projects of the Ministry of Science and Technology of China (2018YFE0115700).

References

- [1] J. Z. Li, J. Q. Zhang, H. Sun, Y. Yang and Y. Xie, "An optical fiber sensor based on carboxymethyl cellulose/carbon nanotubes composite film for simultaneous measurement of relative humidity and temperature," *Optics Communications*, vol. 467, no. 7, pp. 125740, 2020.
- [2] H. Y. Wen, Y. C. Liu and C. C. Chiang, "The use of doped conductive bionic muscle nanofibers in a tennis racket-shaped optical fiber humidity sensor," *Sensors and Actuators B Chemical*, vol. 320, pp. 128340, 2020.
- [3] X. Wang, G. Farrell, E. Lewis, T. Ke, L. Yuan and P. Wang, "A humidity sensor based on a single mode-side polished multimode-singlemode (SSPMS) optical fibre structure coated with gelatin," *Journal of Lightwave Technology*, vol. 18, pp. 1-1, 2017.
- [4] Y. Wei, X. Chen and Z. Jian, "A capacitive humidity sensor based on gold PVA coreshell nanocomposites," *SENSORS AND ACTUATORS B*, vol. 145, no. 1, pp. 327-333, 2010.
- [5] D. Z. Zhang, Y. H. Cao, P. Li, J. F. Wu and X. Q. Zong, "Humidity-sensing performance of layer-by-layer self-assembled tungsten disulfide/tin dioxide nanocomposite," *Sensors & Actuators B Chemical*, vol. 265, pp. 529-538, 2018.
- [6] L. Chen and Z. Jian, "Capacitive humidity sensors based on the dielectrophoretically manipulated ZnO nanorods," *Sensors & Actuators A Physical*, vol. 178, pp. 88-93, 2012.
- [7] D. Zhang, H. Chen, L. Peng, D. Wang and Z. Yang, "Humidity Sensing Properties of Metal Organic Framework-Derived Hollow Ball-Like TiO₂ Coated QCM Sensor," *IEEE Sensors Journal*, vol. 99, pp. 1-1, 2019.
- [8] J. W. Han, B. Kim, J. Li and M. Meyyappan, "Carbon Nanotube Based Humidity Sensor on Cellulose Paper," *The Journal of Physical Chemistry C*, vol. 116, no. 41, pp. 22094-22097, 2012.
- [9] Y. Wang, C. Shen, W. Lou, F. Shentu, C. Zhong, X. Dong and L. Tong, "Fiber optic relative humidity sensor based on the tilted fiber Bragg grating coated with graphene oxide," *Applied Physics Letters*, vol. 109, no. 3, pp. 031107, 2016.
- [10] D. Zhang, J. Tong and B. Xia, "Humidity-sensing properties of chemically reduced graphene oxide/polymer nanocomposite film sensor based on layer-by-layer nano self-assembly," *Sensors and Actuators B: Chemical*, vol. 197, pp. 66-72, 2014.
- [11] D. Zhang, J. Tong, B. Xia and Q. Xue, "Ultrahigh performance humidity sensor based on layer-by-layer self-assembly of graphene oxide/polyelectrolyte nanocomposite film," *Sensors & Actuators B Chemical*, vol. 203, pp. 263-270, 2014.
- [12] B. Jiang, Z. Bi, Z. Hao, Q. Yuan, D. Feng, K. Zhou, L. Zhang, X. Gan and J. Zhao, "Graphene oxide-deposited tilted fiber grating for ultrafast humidity sensing and human breath monitoring," *Sensors and Actuators B: Chemical*, vol. 293, pp. 336-341, 2019.
- [13] Y. Zheng, X. Dong and C. Zhao, "Relative Humidity Sensor Based on Microfiber Loop Resonator," *Advances in Materials Science and Engineering*, vol. 2013, no. 1, pp. 346-349, 2013.
- [14] X. F. Fan, Q. Z. Wang, M. Q. Zhou, F. X. Liu and H. Y. Meng, "Humidity sensor based on a graphene oxide-coated few-mode fiber Mach-Zehnder interferometer," *Optics Express*, vol. 28, no. 17, 2020.
- [15] A. Harith, M. T. Rahman, S. N. A. Sakeh, M. Z. A. Razak and M. Z. Zulkifli, "Humidity sensor based on microfiber resonator with reduced graphene oxide," *Optik - International Journal for Light and Electron Optics*, vol. 127, no. 5, pp. 3158-3161, 2016.
- [16] M. Yang, D. N. Wang and C. R. Liao, "Fiber Bragg grating with micro-holes for simultaneous and independent refractive index and temperature sensing," *IEEE Photonics Technology Letters*, vol. 23, no. 20, pp. 1511-1513, 2011.

- [17] D. R. Dreyer, S. Park, C. W. Bielawski and R. S. Ruoff, "The chemistry of graphene oxide," *Chemical Society Reviews*, vol. 1, 2010.
- [18] O. Leenaerts, B. Partoens and F. M. Peeters, "Adsorption of H₂O, NH₃, CO, NO₂, and NO on graphene: A first-principles study," *Physical Review B*, vol. 77, no. 12, 2008.
- [19] S. Cerveny, F. Barroso-Bujans, A. Alegri and J. Colmenero, "Dynamics of Water Intercalated in Graphite Oxide," *Journal of Physical Chemistry C*, no. 6, pp. 2604-2612, 2010.
- [20] Y. Wang, C. Shen, W. Lou, F. Shentu, C. Zhong, X. Dong and L. Tong, "Fiber optic relative humidity sensor based on the tilted fiber Bragg grating coated with graphene oxide," *Appl. Phys. Lett.*, vol. 109, no. 3, pp. 031107, 2016.
- [21] C. Y. Chao and L. J. Guo, "Reduction of Surface Scattering Loss in Polymer Microrings Using Thermal-Reflow Technique," *IEEE Photonics Technology Letters*, vol. 16, no. 6, pp. 1498-1500, 2004.
- [22] W. S. H. Jr and R. E. Offeman, "Preparation of Graphitic Oxide," *Journal of the American Chemical Society*, vol. 80, no. 6, 1958.
- [23] S. W. Lee, B. I. Choi, J. C. Kim, S. B. Woo and Y. G. Kim, "Reducing individual difference and temperature dependency of QCM humidity sensors based on graphene oxides through normalization of frequency shifts," *Sensors and Actuators B: Chemical*, vol. 313, pp. 128043, 2020.
- [24] J. R. Schwesyg, T. Beckmann and A. S. Zimmermann, "Fabrication and characterization of whispering-gallery-mode resonators made of polymers," *Optics Express*, vol. 17, no. 4, pp. 2573, 2009.
- [25] N. B. Zhong, X. Xin, H. M. Liu, X. Y. Yu and J. Zhao, "Plastic optical fiber sensor for temperature-independent high-sensitivity detection of humidity," *Applied Optics*, vol. 59, no. 19, 2020.
- [26] P. Urbancova, J. Chylek, P. Hlubina and D. Pudis, "Guided-Mode Resonance-Based Relative Humidity Sensing Employing a Planar Waveguide Structure," *Sensors*, vol. 20, no. 23, pp. 6788, 2020.
- [27] Z. X. Hu, C. Y. X. Chen, J. Y. Tian, Z. Y. Yan, Z. H. Weng, M. Gusain, Y. Q. Zhan and L. M. Xiao, "A hybrid self-growing polymer microtip for ultracompact and fast fiber humidity sensing," *Sensors and Actuators: B. Chemical*, vol. 346, pp. 130462, 2021.
- [28] V. V. Genaro, P. G. Cindy, D. B. Beatriz, C. J. Mariel, P. C. Daniel, J. E. Alejandra, E. M. Silvia, L. M. Reyna, C. Remi, M. Laurent, Z. H. Diego and H. Mathieu "Building a microfluidic cell culture platform with stiffness control using Loctite 3525 glue," *Lab on a Chip*, vol. 19, pp. 1-24, 2019.
- [29] H. L. Hampsch, J. Yang, G. K. Wong and J. M. Torkelson, "Thermal degradation of saturated poly (methyl methacrylate)," *Macromolecules*, vol. 21, pp. 528-530, 1988.
- [30] S. W. Lee, B. I. Choi, J. C. Kim, S. B. Woo, Y. G. Kim, S. Kwon, J. Yoo and Y. S. Seo, "Sorption/desorption hysteresis of thin-film humidity sensors based on graphene oxide and its derivative," *Sensors and Actuators B: Chemical*, vol. 273, pp. 575-580, 2016.
- [31] S. Mehrabani, P. Kwong, M. Gupta and A. M. Armani, "Hybrid microcavity humidity sensor," *Applied Physics Letters*, vol. 102, no. 24, pp. 241101, 2013.
- [32] J. Zhang, J. Zhong, Y. F. Fang, J. Wang, G. S. Huang, X. G. Cui and Y. F. Mei, "Roll up polymer/oxide/polymer nanomembranes as a hybrid optical microcavity for humidity sensing," *Nanoscale*, vol. 6, no. 22, pp. 13646-13650, 2014.
- [33] M. A. Gouveia, P. E. S. Pellegrini, J. S. Dos Santos, I. M. Raimundo and C. M. B. Cordeiro, "Analysis of immersed silica optical microfiber knot resonator and its application as a moisture sensor," *Applied Optics*, vol. 53, no. 31, pp. 7454-61, 2014.
- [34] M. Eryürek, Z. Tasdemir, Y. Karadag, S. Anand, N. Kilinc, B. E. Alaca and A. Kiraz, "Integrated Humidity Sensor Based on SU-8 Polymer Microdisk Microresonator," *Sensors and Actuators B: Chemical*, vol. 242, pp. 1115-1120, 2017.
- [35] A. K. Mallik, G. Farrell, D. Liu, V. Kavungal, Q. Wu and Y. Semenova, "A Coated Spherical Microresonator for Measurement of Water Vapor Concentration at PPM Levels in Very Low Humidity Environments," *Journal of Lightwave Technology*, vol. 36, pp. 2667-2674, 2018.
- [36] L. Liang, S. Hao, L. Nan, H. Luo, T. Gang, Q. Rong, X. Qiao and M. Hu, "High-sensitivity optical fiber relative humidity probe with temperature calibration ability," *Applied Optics*, vol. 57, no. 4, pp. 872, 2018.
- [37] A. B. Petermann, T. Hildebrandt, U. Morgner, B. W. Roth and M. Meinhardt-Wollweber, "Polymer Based Whispering Gallery Mode Humidity Sensor," *Sensors*, vol. 18, no. 7, pp. 2383, 2018.
- [38] S. R. Azzuhri, I. S. Amiri, A. S. Zulkhairi, M. A. M. Salim, M. Z. A. Razak, M. F. Khyasudeen, H. Ahmad, R. Zakaria and P. Yupapin, "Application of graphene oxide based Microfiber-Knot resonator for relative humidity sensing," *Results in Physics*, 2018.
- [39] K. Xu, H. Li, Y. Liu, Y. Wang, J. Tian, L. Wang, J. Du, Z. He and Q. Song, "Optical Fiber Humidity Sensor Based on Water Absorption Peak Near 2- μ m Waveband," *IEEE Photonics Journal*, pp. 1-8, 2019.
- [40] M. H. Jali, H. R. A. Rahim, M. A. M. Johari, U. U. M. Ali, S. H. Johari, H. Mohamed, S. W. Harun and M. Yasin, "Formaldehyde sensor with enhanced performance using microsphere resonator-coupled ZnO nanorods coated glass," *Optics and Laser Technology*, vol. 139, pp. 106853, 2021.